A Microwave and Quantum Chemical Study of the Conformational Properties of Etheneselenocyanate ($H_2C{=}CHSeC{\equiv}N$)

Harald Møllendal*,† and Jean-Claude Guillemin‡

Centre for Theoretical and Computational Chemistry (CTCC), Department of Chemistry, University of Oslo, P.O. Box 1033 Blindern, NO-0315 Oslo, Norway, and Sciences Chimiques de Rennes, UMR 6226 CNRS-ENSCR, Ecole Nationale Supérieure de Chimie de Rennes F-35700 Rennes, France

Received: March 5, 2007; In Final Form: May 7, 2007

The structural and conformational properties of etheneselenocyanate ($H_2C{=}CHSeC{\equiv}N$) have been explored by microwave spectroscopy and quantum chemical calculations performed at the MP2/aug-cc-pVTZ and B3LYP/aug-cc-pVTZ levels of theory. The spectra of two rotameric forms were assigned. The more stable form has a synperiplanar conformation, whereas the less stable form has an anticlinal conformation characterized by a C−C−Se−C dihedral angle of 163(3)° from the synperiplanar position (0°). The synperiplanar form was found to be 4.5(4) kJ/mol more stable than the anticlinal form by relative intensity measurements performed on microwave transitions. The spectra of several isotopologues and two vibrationally excited states were assigned for the synperiplanar conformer. The anticlinal rotamer displays a complicated pattern of low-frequency vibrational states, which is assumed to reflect the existence of a small potential hump at the antiperiplanar (180°) conformation. The predictions made in the MP2 and B3LYP calculations are in reasonably good agreement with the experimental results in some cases, whereas rather large differences are seen for other molecular properties.

Introduction

Very few experimental gas-phase studies of structural and conformational properties of organic selenocyanates have been reported. The structure, dipole moment, and barrier to internal rotation of the methyl group of methyl selenocyanate (CH_3SeCN) have been investigated by Sakaizumi et al.[1,2] using microwave (MW) spectroscopy. Rotational isomerism is possible for ethyl selenocyanate (CH_3CH_2SeCN). One conformer, which has a synclinal (*sc*) conformation for the C−C−Se−C chain of atoms, was found in a MW study.[3]

The synthesis of etheneselenocyanate, $H_2C{=}CHSeCN$ (henceforth called ESE), was recently reported,[4] allowing experimental work to be performed on this compound. ESE was characterized by photoelectron and NMR spectroscopies, mass spectrometry, and quantum chemical calculations in this study.[4] These calculations[4] indicate that two rotameric forms exist for ESE. The more stable form was predicted to have a synperiplanar (*sp*) conformation for the C−C−Se−C chain of atoms, whereas the less stable rotamer was calculated to have an anticlinal (*ac*) conformation for this link of atoms. These two conformers are depicted in Figure 1.

The fact that so few conformational studies have been performed for selenocyanates motivated the present work. We also wanted to compare the properties of selenocyanates with those of thiocyanates, which are much better known, to investigate the influence of the selenium atom on the conformational and structural properties. The methods we have used are MW spectroscopy and high-level quantum chemical calculations. MW spectroscopy was chosen because of its high accuracy and resolution, making this method especially suitable for conformational studies of gaseous species. The spectroscopic work has been augmented by high-level quantum chemical calculations, which were conducted with the purpose of obtaining information for use in assigning the MW spectrum and investigating properties of the potential-energy hypersurface.

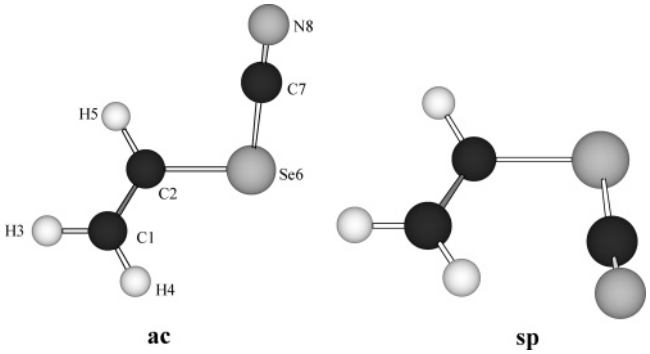

Figure 1. The anticlinal (*ac*) and synperiplanar (*sp*) conformers of $H_2C{=}CHSeC{\equiv}N$ with atom numbering. The MW spectra of both these rotamers were assigned in this work. The *sp* rotamer is 4.5(4) kJ/mol more stable than the *ac* conformer, which has a C1−C2−Se6−C7 dihedral angle of 166(3)° from *sp* (0°).

Experimental Section

Synthesis. *Etheneselenocyanate is malodorous and potentially toxic. All reactions and handling should be carried out in a well-ventilated hood.*

The sample used in this experiment was synthesized and purified as described previously.[4] This experimental procedure is repeated in the Supporting Information for the convenience of the reader.

Microwave Experiment. The MW spectrum was recorded in the 23−80 GHz spectral region using the Stark-modulated spectrometer of the University of Oslo. Individual transitions

* To whom correspondence should be addressed. E-mail: harald.mollendal@kjemi.uio.no.
† University of Oslo.
‡ Ecole Nationale Supérieure de Chimie de Rennes.

10.1021/jp071768+ CCC: $37.00
Published on Web 06/29/2007

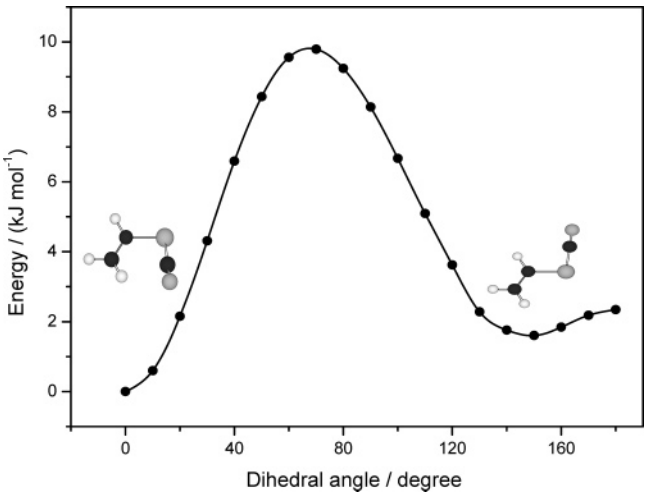

Figure 2. The B3LYP/aug-cc-pVTZ potential function for rotation about the C2−Se6 bond. The values of the C1−C2−Se6−C7 dihedral angle are given on the abscissa. A dihedral angle of 0° corresponds to the *sp* conformer, which is sketched on the left side of figure, whereas a dihedral angle of 148° corresponds to the *ac* rotamer (right). The observations are only in qualitative agreement with these predictions; see text.

were measured with an estimated accuracy of ∼0.15 MHz. Details of the construction and operation of this device, which has a 2 m Hewlett-Packard Stark cell, have been given elsewhere.[5,6] The cell was cooled to roughly −20 °C while recording the spectrum in the 23−40 GHz region to enhance the intensity of the spectral lines. Lower temperatures, which would have increased the intensity of the spectrum even more, could not be achieved, due to insufficient vapor pressure of ESE. The spectrum in the 40−80 GHz interval is considerably stronger than at lower frequencies and was therefore recorded mostly at room temperature. Radio frequency microwave double resonance experiments (RFMWDR), similar to those performed by Wodarczyk and Wilson,[7] were also conducted to assign unambiguously particular transitions.

Results

Quantum-Chemical Calculations. The present ab initio and density functional theory (DFT) calculations were performed employing the Gaussian 03 suite of programs,[8] running on the 64 processor HP "superdome" computer in Oslo. Electron correlation was taken into consideration in the ab initio calculations using the Møller-Plesset second-order perturbation calculations (MP2).[9] Becke's three-parameter hybrid functional[10] employing the Lee, Yang, and Parr correlation functional[11] (B3LYP) was employed in the DFT calculations. Dunning's[12] correlation-consistent triple-ζ basis set, aug-cc-pVTZ, which includes polarized functions for the valence electrons and is augmented by additional diffuse functions, was used throughout this work. Our MP2 and B3LYP/aug-cc-pVTZ calculations are at a somewhat higher level of theory than those of Bajor et al., who conducted calculations at the MP2 and B3LYP/cc-pVTZ levels.[4]

Rotation about the C2−Se6 bond (Figure 1) produces rotational isomerism for ESE. B3LYP/aug-cc-pVTZ calculations of the energies were therefore performed for the 0° to 180° interval in steps of 10° of the C1−C2−Se6−C7 dihedral angle, employing the scan option of the Gaussian 03 program, allowing all remaining structural parameters to vary freely. The resulting potential function shown in Figure 2 indicates that there are two minima (two "stable" conformers) of the potential energy hypersurface at about 0° (*sp*) and 148.1° (*ac*) for the C1−C2−Se6−C7 dihedral angle, with an energy difference of about 1.60 kJ/mol, with *sp* as the more stable conformer. This function has maxima at 70° (9.79 kJ/mol above the energy of *sp*) and at 180° (2.34 kJ/mol above the energy of *sp*). The barrier of transformation from the +*ac* to its mirror image, the −*ac* conformer, is as low as 0.74 kJ/mol. This barrier has its maximum at the exact antiperiplanar (*ap*) conformation (180°).

Separate B3LYP calculations of the energies and vibrational frequencies were then performed for the *sp* and *ac* rotamers. The starting values of the C1−C2−Se6−C7 dihedral angles were chosen to be close to 0° and 150°, respectively. Full geometry optimizations with no symmetry restrictions were undertaken employing the default convergence criteria of Gaussian 03. The *sp* conformer was found to have a symmetry plane (C_s symmetry) with the said dihedral angle being exactly 0°. The C1−C2−Se6−C7 dihedral angle was found to be 148.1° in the *ac* rotamer. Only positive values were found for the vibrational frequencies, as expected for these two minima on the potential energy hypersurface. The electronic energy difference corrected for zero-point vibrational contributions was calculated to be 1.20 kJ/mol with *sp* as the more stable rotamer, as compared to the uncorrected value of 1.60 kJ/mol referred to above.

Analogous MP2 calculations were repeated for the *sp* and *ac* rotamers. The *sp* form was again found to have exact C_s symmetry, whereas the C1−C2−Se6−C7 dihedral angle was predicted to be 137.8° in the *ac* conformer, about 10° less than that found in the B3LYP calculations. The vibrational frequencies found in these calculations are listed in Table 13S in the Supporting Information. The energy difference corrected for zero-point vibrational effects was predicted to be 4.02 kJ/mol with *sp* as the more stable in this case. The B3LYP and MP2 results for the energy difference between the two forms therefore vary by 2.8 kJ/mol, which are not unexpected given the large number of electrons (62) involved in these calculations.

The MP2 and B3LYP geometries are listed in Table 1, while additional parameters obtained in these calculations for the most abundant isotopologue ($H_2C{=}CH^{80}SeCN$; ^{80}Se occurs with 49.8% relative abundance) are displayed in Table 2, which also contains experimental results obtained for the ground vibrational states of both *sp* and *ac* for convenient comparison with the theoretical predictions. The principal axis coordinates calculated from the B3LYP structure are given in Table 3, and projections of the *ac* and *sp* rotamers in the *a*−*b* principal inertial axis system are shown in Figure 3.

Comparison of the MP2 and B3LYP structural results (Table 1) reveals that the structure of the vinyl ($H_2C{=}CH$) group is predicted to be similar in the two methods, because the bond lengths and bond angles agree to within about 1 pm and 1°, respectively. There are relatively larger disagreements between C2−Se6, Se6−C7, and C7≡N8 MP2 and B3LYP bond lengths, which differ by about 2−2.5 pm. The values of the C1−C2−Se6 angle agree to within approximately 1°, whereas a discrepancy of about 2° is seen for the C2−Se6−C7 angle. Interestingly, both methods find that the C1−C2−S6 angle in the *sp* form opens up by about 6° in comparison with the same angle in the *ac* rotamer, which may indicate that repulsion between the vinyl and selonocyanate group may play a role. The rather large difference (10.3°) in the C1−C2−Se6−C7 dihedral angle has been alluded to above.

There are few experimental structures reported for selenocyanates for comparison with the present calculations. However, in the substitution structure (r_s)[13] of methyl selenocyanate,[2] the

TABLE 1: MP2 and B3LYP Geometries[a] of the *ac* and *sp* Conformers of $CH_2{=}CHSeC{\equiv}N$

method:	MP2		B3LYP	
conformer:	*ac*	*sp*	*ac*	*sp*
	Bond Length (pm)			
C1−C2	133.3	133.2	132.3	132.2
C1−H3	108.1	108.1	108.2	108.2
C1−H4	108.1	108.2	108.2	108.1
C2−H5	108.1	108.3	108.0	108.2
C2−Se6	189.9	189.8	192.7	192.4
Se6−C7	182.8	182.1	184.7	184.3
C7−N8	117.7	117.7	115.5	115.5
	Angle (deg)			
C2−C1−H3	120.0	119.2	120.1	119.6
C2−C1−H4	121.8	122.4	122.8	123.0
H3−C1−H4	118.2	118.5	117.1	117.5
C1−C2−H5	123.2	122.4	123.8	123.1
C1−C2−Se6	120.7	126.6	121.5	127.7
H5−C2−Se6	116.0	111.0	114.6	109.2
C2−Se6−C7	95.7	96.2	97.2	98.4
Se6−C7−N8	178.6	179.1	177.8	178.9
	Dihedral Angle[b] (deg)			
H3−C1−C2−H5	0.8	0.0	0.9	−0.0
H3−C1−C2−Se6	−174.3	180.0	−174.6	−180.1
H4−C1−C2−H5	−179.4	−180.0	−179.3	−179.9
H4−C1−C2−Se6	5.5	0.0	5.2	−0.0
C1−C2−Se6−C7	−137.8	0.0	−148.1	−0.0
H5−C2−Se6−C7	46.8	−180.0	36.0	179.9
C2−Se6−C7−N5	−151.4	0.2	−161.2	179.0

[a] aug-cc-pVTZ basis set. [b] Measured from $sp = 0°$.

C−Se bond length of the selenocyanate group is 183.6(11) pm, a bit longer than the MP2 values for the Se6−C7 bond length and somewhat shorter than the B3LYP distance shown in Table 1. The C≡N bond length in methyl selenocyanate is 116.2(9) pm,[2] which is somewhat shorter than the MP2 value, but longer than the B3LYP prediction for the C7≡N8 bond (Table 1). The equilibrium bond length of this functional group is not expected to be accurately predicted by the methods of calculations employed in this work.

The differences between the MP2 and B3LYP geometries result in variations of several (∼3−8) percent in the predicted values of the rotational constants, as seen from Table 2. The A-reduction quartic centrifugal distortion constants[13] predicted by the two theoretical methods differ significantly, and the B3LYP dipole moment components are generally smaller or similar to their MP2 counterparts (Table 2). The MP2 calculations predict that the *sp* rotamer is favored by 4.0 kJ/mol over the *ac* form after corrections for zero-point vibrational energies, whereas B3LYP calculations find this energy difference to be 1.2 kJ/mol (Table 2).

MW Spectrum and Assignment of *sp*. Selenium has six naturally occurring isotopes. Five of these are relatively abundant, ^{76}Se (9.0%), ^{77}Se (7.6%), ^{78}Se (23.5%), ^{80}Se (49.8%), and ^{82}Se (9.2%). The quantum chemical calculations above indicate that the rotational constants of the two forms are relatively small and that there are about five vibrational fundamentals with frequencies below 500 cm^{-1} for each rotamer (not given in Table 1 or 2). The two lowest fundamental frequencies of each conformer are the C2−Se6 torsional frequency and the lowest bending vibration. The B3LYP calculations (uncorrected) predict the bending vibration to be 120 cm^{-1} and the C3−Se6 torsional vibration to be 122 cm^{-1} in the *sp* conformer. The corresponding values in *ac* are 120 and 59 cm^{-1}, respectively. All of this means that ESE will have a relatively large partition function and each quantum state will therefore have a comparatively low population, resulting in a relatively weak MW spectrum. Cooling of the Stark cell reduces the partition function and enhances spectral intensities. It is unfortunate that ESE has a comparatively low vapor pressure, which made it impossible to investigate the MW spectrum at temperatures lower than approximately −20 °C, using our equipment.

The MW spectrum of ESE turned out to be comparatively weak and extremely dense with absorption lines occurring every few MHz, as expected. The lines were relatively broad due to relatively large dipole moments of each rotamer (Table 3) and unresolved nuclear quadrupole hyperfine structure cause by the ^{14}N nucleus. This is the reason why the spectral accuracy is no better than ±0.15 MHz.

Both the MP2 and the B3LYP calculations predict that the *sp* conformer is the preferred form of the molecule by 4.0 (MP2) or 1.2 kJ/mol (B3LYP) (Table 2). It is seen from Table 2 that the dipole moment of *sp* is predicted to have its largest component along the *a*-principal inertial axis ($\sim 12 \times 10^{-30}$ C m). The strongest transitions of its spectrum are therefore the a-type R-branch transitions. Searches were first made for the spectrum of the most abundant isotopologue, $H_2C{=}CH^{80}SeCN$, which is an oblate rotor with Ray's asymmetry parameter[14] $\kappa = 0.36$. These transitions were soon found. Their assignments were confirmed by their Stark effects and fit to Watson's A-reduction Hamiltonian using the I^r-representation.[15] The assignments were then extended to include the a-type Q-branch transitions as well. About 300 transitions were assigned in this manner. The hypothetical frequencies of b-type lines could be predicted accurately from these a-type lines, but none was identified with 100% certainty, due to their relatively low intensity, with the high spectral density as an additional difficulty. The reason for the relatively low intensity of the b-type transitions is assumed to be the fact that the *b*-axis dipole moment component has roughly 50% of the value of the *a*-axis component (Table 2) and the fact that MW intensities are proportional to the μ^2.

Two hundred and eight-four lines with a maximum value of $J = 60$ and $K_{+1} = 24$ (see the Supporting Information; Table 3S) were used to derive the spectroscopic constants shown in Tables 2 and 4. One sextic centrifugal distortion constant, Φ_{JK}, had to be used in addition to the five quartic centrifugal distortion constants to get a satisfactory fit with a root-mean-square deviation comparable to the experimental uncertainty of ±0.15 MHz.

Changes in the rotational constants upon isotopic substitution from the values obtained for the ^{80}Se isotopologue were calculated employing the B3LYP structure (Table 2). These changes were used to predict the rotational constants of the ^{76}Se, ^{78}Se, and ^{82}Se isotopologues, whose spectra were found close to their predicted frequencies. The spectroscopic constants of these species are shown in Table 4, and the spectra are listed in the Supporting Information, Tables 1S, 2S, and 4S. Only the strong ^{a}R-transitions were assigned for $H_2C{=}CH^{76}SeCN$ and $H_2C{=}CH^{82}SeCN$, due to their low relative abundance. The Δ_K, δ_J, δ_K, and Φ_{JK} centrifugal distortion constants were therefore preset in the least-squares fit at the values found for the parent ($H_2C{=}CH^{80}SeCN$) isotopologue.

Inspection of Tables 2 and 4 reveals that there are large differences between the theoretical and experimental quartic centrifugal distortion constants, especially for δ_J and δ_K. Even the advanced calculations used in the present case therefore fail to predict a reliable force field for the *sp* conformer of ESE.

A small and positive inertial defect defined by $\Delta = I_c - I_a - I_c$ is generally observed for planar molecules.[16−18]

TABLE 2: Rotational Constants,[a] Inertial Defect,[b] Watson's A-Reduction Centrifugal Distortion Constants,[c] Principal Axis Dipole Moment Components, and Energy Differences of Conformer *ac* and Conformer *sp* of $H_2C{=}CH^{80}SeC{\equiv}N$

method:	MP2		B3LYP		experimental	
conformer:	*ac*	*sp*	*ac*	*sp*	*ac*	*sp*
			Rotational Constants (MHz)			
A	6712.5	4046.8	7229.6	4149.6	7170.89(18)	4077.2227(27)
B	2282.6	3475.2	2182.8	3252.0	2230.432(13)	3392.5379(22)
C	1761.1	1869.6	1711.2	1823.2	1729.922(14)	1849.7425(20)
			Inertial Defect[a] (10^{-20} u m^2)			
Δ^a	−34.756	0.0[d]	−21.773	0.0[d]	−4.9201(51)	0.29627(22)
			Centrifugal Distortion Constants[c] (kHz)			
Δ_J	1.18	3.32	0.844	3.09	1.1064(38)	5.1985(60)
Δ_{JK}	−17.5	−13.3	−14.4	−13.1	−18.341(10)	−16.093(16)
Δ_K	115	15.2	123	16.5	123[d]	11.053(14)
δ_J	0.437	1.57	0.287	1.45	0.329(12)	−0.0535(15)
δ_K	−0.620	−1.21	0.0574	−0.836	0.0574[d]	−17.456(20)
			Principal Axes Dipole Moment Components[e] (10^{-30} C m)			
μ_a	15.0	12.0	14.0	11.5	*f*	*f*
μ_b	3.4	5.6	3.4	6.2	*f*	*f*
μ_c	1.0	0.0[g]	1.0	0.0[g]	*f*	*f*
			Energy Difference[h] (kJ/mol)			
ΔE	4.0	0.0	1.2	0.0	4.5(4)	0.0

[a] The aug-cc-pVTZ basis set was used in the MP2 and B3LYP calculations. [b] $\Delta = I_c - I_a - I_b$, where I_a, I_b, and I_c are the principal moments of inertia. Conversion factor 505379.05 MHz u 10^{-20} m^2. [c] A-reduction I^r-representation.[15] [d] Fixed; see text. [e] 1 Debye = 3.33564×10^{-30} C m. [f] Not measured. [g] For symmetry reasons. [h] The energy of the *sp* conformer is assigned a value of 0 kJ/mol.

TABLE 3: B3LYP Principal-Axis Coordinates of $H_2C{=}CH^{80}SeC{\equiv}N$

conformer:	*ac*			*sp*[a]	
coordinates (pm):	*a*	*b*	*c*	*a*	*b*
C1	−248.5	−85.6	−21.5	144.0	187.7
C2	−125.4	−90.1	26.6	152.3	55.8
H3	−318.6	−164.8	1.4	234.6	246.8
H4	−284.2	−4.8	−83.9	49.8	240.7
H5	−87.8	−170.6	88.2	246.5	2.5
Se6	−2.1	55.8	1.4	7.7	−71.2
C7	152.4	−45.2	−5.2	−132.8	48.1
N8	251.3	−104.6	−8.5	−222.2	121.2

[a] The *c*-coordinates are zero by symmetry.

It is seen from Table 4 that the inertial defect varies from about 0.289 to 0.309 $\times$ 10^{-20} u m^2 for the four isotopologues. This is similar to the inertial defect found for the sulfur congener, $H_2C{=}CHSCN$ (0.22347(56) $\times$ 10^{-20} u m^2), which was assumed to be planar.[19,20] It is therefore concluded that *sp* conformer of ESE has a planar equilibrium structure in agreement with the B3LYP and MP2 calculations.

Vibrationally Excited States of *sp*. The spectra of two vibrationally excited states of $H_2C{=}CH^{80}SeCN$ were also assigned. The spectroscopic constants are shown in the two last columns of Table 4, and the spectra are listed in the Supporting Information, Tables 5S and 6S.

The inertial defect of one of these vibrationally excited states is seen to be negative (−1.4651(12) $\times$ 10^{-20} u m^2). The decrease of the inertial defect upon excitation is typical for an out-of-plane vibration.[16,17] It is therefore assumed that this is the first excited state of the torsion about the C2−Se6 bond. Relative intensity measurements performed as described by Esbitt and Wilson[21] yielded 120(20) cm^{-1} for this vibration, close to the B3LYP (not given in Table 1 or 2) and the MP2 (Supporting Information; Table 13S) result of 123 and 130 cm^{-1}, respectively.

The inertial defect of the vibrationally excited state, whose spectroscopic constants are listed in the last column of Table 4, is positive (2.2177(12) $\times$ 10^{-20} u m^2). This is typical for an in-plane bending vibration.[16,17] Relative intensity measurements yielded 136(25) cm^{-1} for this fundamental as compared to 120 (B3LYP) and 127 cm^{-1} (MP2). The lowest torsional and in-plane bending vibrations therefore have very similar frequencies of 120(20) and 136(25) cm^{-1}. The theoretical calculations predict that there is insignificant Coriolis interaction between the two fundamentals. This is in accord with the finding that the spectra of these two states can be fitted to the Watson Hamiltonian[15] to within the experimental accuracy of ±0.15 MHz.

Further vibrationally excited states of this conformer have frequencies above ∼325 cm^{-1} according to the theortical calculations (Table 13S; Supporting Information), which would result in very weak lines that were not assigned.

Structure of the *sp* Conformer. The rotational constants in Table 4 furnish insufficient information for a full determination of the structure of this planar rotamer. Comparison of the theoretical rotational constants with the experimental rotational constants (Table 2) shows that the MP2 rotational constants are somewhat closer to the experimental values than the B3LYP rotational constants are, but this could be fortuitous and does not necessarily reflect that the MP2 structure is more accurate than the B3LYP structure. It is conjectured that the bond lengths and bond angles obtained in both calculation procedures represent the equilibrium values to within 2 pm and 2°, respectively.

Assignment of the MW Spectrum of the *ac* Conformer. The *ac* rotamer is a prolate rotor with the asymmetry parameter $\kappa = -0.8$,[14] according to the theoretical predictions (Table 2). This conformer is calculated to have a predominating component of the dipole moment as large as ∼14−15 $\times$ 10^{-30} C m along the *a*-axis (Table 2). The a-type R-branch transitions are therefore predicted to be the strongest lines in the spectrum of this rotamer. The 40−80 GHz spectral interval was first investigated. The rotational constants (Table 2) predict that ^{a}R-transitions with the principal quantum number *J* between about 10 and 20 occur in this spectral region.

Pairs of ^{a}R-lines with the same K_{-1}-value coalesce for the highest values of K_{-1}. This coalescence results in a very rapid

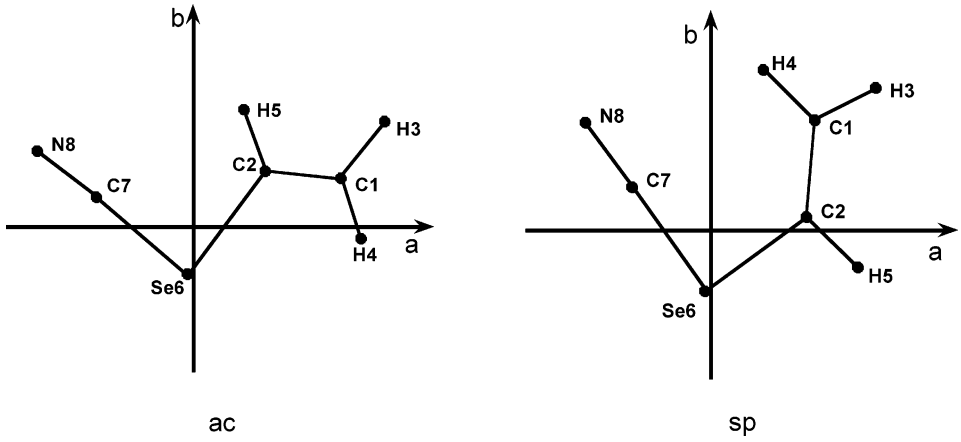

Figure 3. The *ac* and *sp* conformers of $H_2C{=}CHSeCN$ projected in the $a-b$ principal inertial axis plane.

TABLE 4: Experimental Spectroscopic Constants[a] for the *sp* Conformer of $H_2C{=}CHSeC{\equiv}N$

species:	$H_2C{=}CH^{76}SeCN$	$H_2C{=}CH^{78}SeCN$	$H_2C{=}CH^{80}SeCN$	$H_2C{=}CH^{82}SeCN$	$H_2C{=}CH^{80}SeCN^b$	$H_2C{=}CH^{80}SeCN^c$
A (MHz)	4146.759(36)	4111.1496(28)	4077.2227(27)	4044.380(48)	4066.242(15)	4121.808(25)
B (MHz)	3394.232(11)	3393.4396(24)	3392.5379(22)	3392.179(21)	3363.9984(92)	3397.272(12)
C (MHz)	1846.4837(42)	1856.9670(18)	1849.7425(20)	1842.759(10)	1850.8459(36)	1847.2202(31)
Δ_J (kHz)	4.771(33)	5.3097(66)	5.1985(60)	5.459(59)	4.231(49)	6.135(46)
Δ_{JK} (kHz)	−15.656(38)	−16.583(15)	−16.093(16)	−16.394(75)	−15.197(50)	−17.141(48)
Δ_K (kHz)	11.053[d]	11.422(14)	11.053(14)	11.053[d]	11.053[d]	11.053[d]
δ_J (kHz)	−0.0535[d]	−0.0353(15)	−0.0535(15)	−0.0535[d]	−0.0535[d]	−0.0535[d]
δ_K (kHz)	−17.46[d]	−17.522(17)	−17.456(20)	−17.46[d]	−31.10(19)	−4.32(16)
Φ_{JK} (Hz)	−0.0247[d]	−0.03293(59)	−0.02470(60)	−0.0247[d]	−0.0247[d]	−0.0247[d]
Δ^e (10^{-20} m^2 u)	0.2890(15)	0.29580(20)	0.29627(22)	0.3093(35)	−1.4651(12)	2.2177(12)
rms[f] (MHz)	0.152	0.157	0.202	0.202	0.167	0.134
no.[g]	52	199	284	28	86	70

[a] A-reduction I^r-representation.[15] Uncertainties represent one standard deviation. [b] First vibrationally excited state of the torsion about the C2−Se6 bond. [c] First excited state of the lowest bending vibration. [d] Fixed at the value found for the $H_2C{=}CH^{80}SeCN$ isotopologue. [e] Inertial defect defined by $\Delta = I_c - I_a - I_b$. Conversion factor: $505379.05 \times 10^{-20}$ MHz u m^2. [f] Root-mean-square deviation. [g] Number of transitions used in the fit.

Stark effect for the said transitions. This spectral behavior was exploited to obtain the first assignments of the MW spectrum of *ac*.

When the spectrum in the 40−80 GHz was scanned using a comparatively low field strength of about 50 V/cm, pile-ups of lines protruded from the background at intervals of approximately 3.9 GHz. These pile-ups are unusually rich in lines and are several hundred MHz wide. A similar observation was made for the *ac* conformer of the sulfur analogue, $H_2C{=}CHSC{\equiv}N$,[19,20] and was ascribed to the presence of a potential hump at the *ap* position resulting in the existence of several vibrationally excited states caused by low-frequency C−S torsional vibrations.[19,20]

Some of these pile-ups of ESE were subsequently studied using the RFMWDR technique[7] to assign particular transitions. A portion of the spectrum of the ^aR $J = 15 \leftarrow 14$ transitions using a radio frequency of 5.05 MHz is shown in Figure 4. This radio frequency modulates the $J = 15_6 \leftarrow 14_6$ pair of lines, which are split by roughly 10 MHz. Five series of lines belonging to various vibrational states (denoted by Roman numerals I−IV) were first assigned in this manner. These transitions were then fitted to Watson's A-reduction Hamiltonian[15] and used to predict the frequencies of additional lines. The comparatively high-K_{-1} lines were then readily assigned because they are modulated at low Stark field strengths. An example is shown in Figure 5. In this portion of the spectrum, the K_{-1} coalescing pair of lines between 13 and 7 of the $J = 14 \leftarrow 13$ transition of the vibrational state denoted by the Roman numeral I is shown.

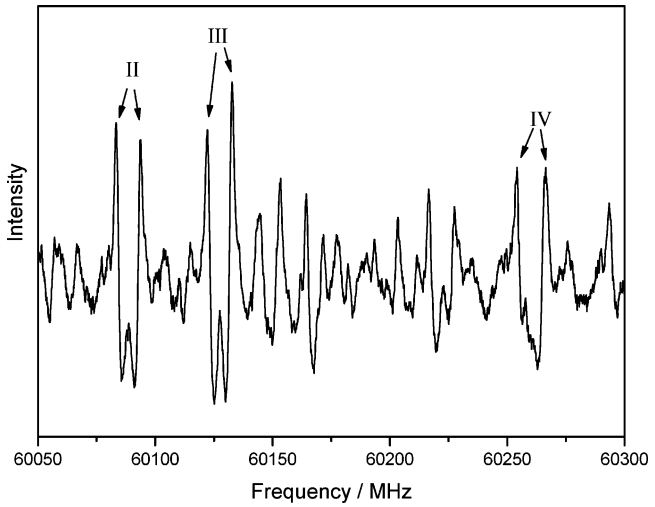

Figure 4. A portion of the RFMWDR spectrum of $J = 15 \leftarrow 14$ transition of the *ac* conformer of $H_2C{=}CHSeCN$ obtained employing a radio frequency of 5.05 MHz. The spectrum shows the $J = 15_6 \leftarrow 14_6$ pair of lines associated with three of the five vibrational states that were assigned for this conformer. A Roman numeral indicates each state. Note the small intensity difference between states II and III.

Assignments of low-K_{-1} transitions have to be made at much higher field strengths than ∼50 V/cm to modulate them. While practically all of the observed lines belong to the *ac* conformer at low field strengths of ∼50 V/cm, the very rich spectrum belonging to the *sp* rotamer gradually becomes modulated as the field strength increases adding a large amount of additional

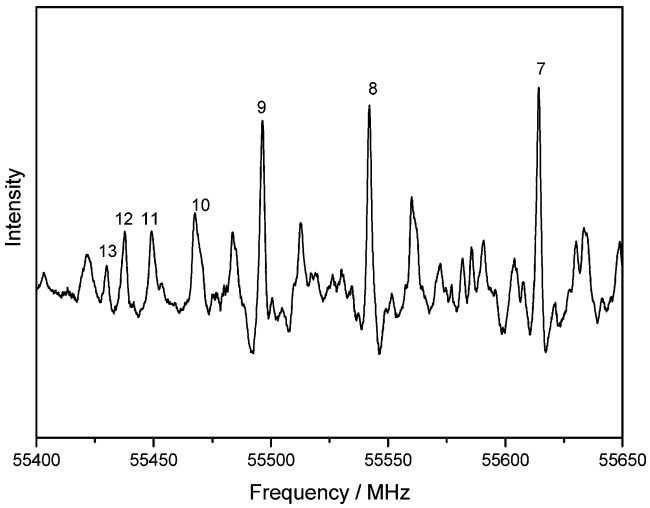

Figure 5. A portion of the MW spectrum showing the $J = 14 \leftarrow 13$ transitions of the vibrational state denoted I. The values of the coalescing K_{-1} lines are shown above each assigned transition.

lines to the spectrum. This often made it difficult to unambiguously assign transitions of the *ac* conformer with K_{-1} less than 4 or 5, because field strengths much higher than 50 V/cm are necessary to modulate them.

The spectra of all five vibrational states could be fitted to the A-reduced Watson Hamiltonian[15] with a root-mean-square deviation comparable to the experimental uncertainty, with the exception of a few high-K_{-1} lines, which have been omitted in the least-squares fit. This failure is possibly caused by higher-order rotation−vibration interactions.

Attempts to find b- and c-type transitions failed, presumably because the corresponding dipole moment components are much less than μ_a (Table 2). The spectra depend very little on the Δ_K and δ_K centrifugal distortion constants, and these constants were fixed at the values obtained in the B3LYP calculations (Table 2) in the least-squares fits. The spectra are listed in the Supporting Information (Tables 7S−11S), and the spectroscopic constants are shown in Table 5. Interestingly, the experimental values of the fitted centrifugal distortion constants Δ_J, Δ_{JK}, and δ_J are in much better agreement (Tables 2 and 5) with the theoretical values in this case than in the case of *ap*.

The fact that there are several relatively abundant isotopes of selenium (see above) made it necessary to explore whether any of the assigned spectra belonged to isotopologues other than the parent isotopologue ($H_2C{=}CH^{80}SeCN$). The B3LYP (Table 1) structure was used for this purpose to predict rotational constants of various isotopologues, which were compared to the rotational constants in Table 5. It was concluded that the spectra of the five states (I−V) must belong to various vibrational states of the parent isotopologue ($H_2C{=}CH^{80}SeCN$) and not to further isotopologues.

Relative intensity measurements were then performed following Esbitt and Wilson.[21] The spectra of two states, denoted II and III, had almost the same intensity at room temperature, as seen in Figure 4. These two spectra were the two strongest ones observed for this conformer. Closer scrutiny revealed that the spectrum of state II tends to be slightly stronger than the spectrum of III, and state II is therefore assumed to be the ground vibrational state, whereas state III is the first excited vibrational state. It was not possible to perform very accurate relative intensity measurements, due to the high spectral density. However, such measurements[21] yielded a vibrational frequency of 21(20) cm^{-1} for II, much lower than the uncorrected values of 59 (B3LYP) and 65 cm^{-1} (MP2). The experimental values found for the torsional vibrations by relative intensity measurements are listed in the last line of Table 5. The frequencies of the three additional vibrationally excited states were determined in the same manner to be 56(30) cm^{-1} for I, 60(30) cm^{-1} for IV, and 93(40) cm^{-1} for V (Table 5). All of these frequencies are lower than the predicted value of the lowest bending vibration (120 (B3LYP) and 128 cm^{-1} (MP2)), which is the second lowest vibration predicted for this conformer.

The irregular pattern formed by the vibrationally excited states of this rotamer is a strong indication that there is a hump at the (*ap*) conformation (which has C_s symmetry) with an associated double minimum potential. This potential cannot be high. The B3LYP calculations yielded a barrier height of 0.74 kJ/mol and a torsional frequency of 59 cm^{-1} (see above). The experimental data indicate that the barrier height is definitely less than the B3LYP prediction and that extensive tunneling through this barrier takes place.

Attempts were subsequently made to fit the available data of the ground and vibrationally excited states of the C2−Se6 torsion of the *ac* conformer using a reduced potential function of the form $V(z) = A(\langle z^4\rangle + B\langle z^2\rangle)$, as suggested by Gwinn and co-workers.[22] The computer program by Møllendal[23] was employed for this purpose. *A* and *B*, as defined by Gwinn,[22] are parameters to be fitted (not to be confused with the rotational constants). *A* may have the dimension cm^{-1}. *B* and *z* are dimensionless. A double minimum potential with a hump at the *ap* conformation will exist if *B* is negative, resulting in C_1 symmetry for the equilibrium conformation of the *ac* rotamer. However, we were not able to get a satisfactory fit to this potential function using the data in Table 5, possibly because Gwinn's procedure[22] is too simplistic in the present case.

The intensity of the spectrum of the $H_2C{=}CH^{78}SeCN$ isotopologue should be about one-half the intensity of the spectrum of the parent species $H_2C{=}CH^{80}SeCN$ (see above). The rotational constants of $H_2C{=}CH^{78}SeCN$ were predicted in the same manner as described above for the *sp* conformer. A series of lines (see Table 12S in the Supporting Information), denoted series VI in Table 5, were tentatively assigned as the ground vibrational state of $H_2C{=}CH^{78}SeCN$. This series partly overlap with series III of $H_2C{=}CH^{80}SeCN$, which complicated the assignment procedure of this isotopologue. The *B* rotational constant was fixed in the fit, because it is easy to predict an accurate value for this constant of this species because the Se atom is close to the *b*- and *c*-inertial axes (Table 3 and Figure 3) and its mass is relatively high.

Structure of the *ac* Conformer. The pattern of the vibrational states observed for this rotamer strongly indicates that this rotamer has a nonplanar equilibrium conformation. The experimental rotational constants of this conformer are in somewhat better agreement with B3LYP than with the MP2 predictions (Tables 2 and 5). Bond lengths and bond angles predicted by the two theoretical approaches presumably represent the equilibrium structure to within 2 pm and 2°, as in the case of the *sp* form.

However, the important C1=C2−Se6−C7 dihedral angle (Table 1) calculated to be 137.8° (MP2) and 148.1° (B3LYP) seems to be predicted far too small in both cases. This can best be shown by comparing the experimental (−4.9201(51)) and theoretical inertial defects (−34.756 (MP2) and -21.773×10^{-20} u m^2 (B3LYP)) shown in Table 2. The inertial defect would have been exact zero, if a completely rigid and planar *ap* conformation had existed for this rotamer. The small value of $-4.9201(51) \times 10^{-20}$ u m^2 for the inertial defect is another indication that the *ac* conformer is nearly but not exactly planar.

TABLE 5: Spectroscopic Constants[a] for the *ac* Conformer of $H_2C{=}CHSeC{\equiv}N$

series:[b]	I	II	III	IV	V	VI
A (MHz)	7136.4(23)	7170.89(18)	7127.28(22)	7045.0(11)	7096.1(16)	7243.4(76)
B (MHz)	2215.46(13)	2230.432(13)	2230.632(10)	2235.165(67)	2247.068(77)	2230.43[d]
C (MHz)	1727.04(15)	1729.922(14)	1732.373(12)	1735.245(82)	1736.461(92)	1733.771(41)
Δ_J (kHz)	1.286(21)	1.1064(38)	1.0849(43)	0.793(14)	1.305(49)	1.126(26)
Δ_{JK} (kHz)	−16.473(48)	−18.341(10)	−17.166(10)	−18.212(42)	−18.123(49)	−18.685(57)
Δ_K (kHz)	123[c]	123[c]	123[c]	123[c]	123[c]	123[c]
δ_J (kHz)	0.65(10)	0.329(12)	0.214(15)	0.274(59)	−0.056(59)	0.19(17)
δ_K (kHz)	0.0574[c]	0.0574[c]	0.0574[c]	0.0574[c]	0.0574[c]	0.0574[c]
Δ[e] (10^{-20} m^2 u)	−6.305(61)	−4.9201(51)	−5.7445(47)	−6.596(31)	−5.085(38)	−4.864[f]
rms[g] (MHz)	0.200	0.190	0.173	0.146	0.207	0.184
no.[h]	53	133	138	45	57	49
vib. frequency (cm^{-1})	56(30)	0	21(20)	60(30)	93(40)	0

[a] A-reduction I^r-representation.[15] Uncertainties represent one standard deviation. [b] The Roman numerals I−IV refer to the ^{80}Se isotopologue, while VI refers to the ^{78}Se isotopologue in the ground vibrational state; see text. [c] Fixed at the value found in the B3LYP calculations; see Table 2. [d] Fixed; see text. [e] Inertial defect defined by $\Delta = I_c - I_a - I_b$. Conversion factor: $505379.05 \times 10^{-20}$ MHz u m^2. [f] No uncertainty limit is given here because the B rotational constant has been fixed in the least-squares fit. [g] Root-mean-square deviation. [h] Number of transitions used in the fit.

The C1=C2−Se6−C7 dihedral angle was then fitted to reproduce the observed inertial defect. Both the MP2 and the B3LYP structures were used in these procedures. A C1=C2−Se6−C7 dihedral angle of 166(3)° yielded the best fit in each case.

Internal Energy Difference between the *ac* and *sp* Conformers. The internal energy difference between two conformers has been derived using a variant of eq 3 of Esbitt and Wilson.[21] According to Wilson,[24] the internal energy difference is given by

$$E''_{v''} - E'_{v'} = E'_{J'} - E''_{J''} + RT \ln L \qquad (1)$$

where $E''_{v''}$ and $E'_{v'}$ are the internal energies of the two conformers in the v'' and v' vibrational states, respectively, $E'_{J'}$ and $E''_{J''}$ are the lowest energy levels of the two rotational transitions under investigations, R is the universal gas constant, and T is the absolute temperature. L is given by

$$L = \frac{S'}{S''}\frac{g''}{g'}\left(\frac{\nu''\mu''}{\nu'\mu'}\right)^2 \frac{l''}{l'}\frac{\Delta\nu'}{\Delta\nu''}\frac{\lambda''}{\lambda'}\frac{(2J'+1)}{(2J''+1)} \qquad (2)$$

where S is the peak signal amplitude of the radiation-unsaturated line, g is the degeneracy other than the rotational degeneracy, which is $2J + 1$, ν is the frequency of the transition, μ is the principal-axis dipole moment component, l is the radiation wave length in the Stark cell,[25] $\Delta\nu$ is the line breadth at half-height, λ is the line strength, and J is the principal rotational quantum number.

The internal energy difference between the ground vibrational states of the *ac* and *sp* conformers was determined by comparing the intensities of several selected ground-state transitions of each conformer. The lines employed in this comparison procedure were relatively strong and not detectably overlapped by other lines. The intensity comparison was performed as described by Esbitt and Wilson.[21] The statistical weight (g) of the *ac* conformer was assumed to be twice the weight of the *sp* rotamer. The radiation wavelengths (l) were assumed to be identical. The line breadths ($\Delta\nu$) were assumed to be proportional to the principal-axis dipole moment component. The ratio of the dipole moment components of the two forms was calculated using the B3LYP predictions in Table 2.

The internal energy difference, $E_{ac} - E_{sp}$, obtained this way varied between 4.2 and 5.3 kJ/mol (*sp* more stable than *ac*) in the six comparisons that were performed. The average value was found to be $E_{ac} - E_{sp} = 4.5$ kJ/mol. There are several sources of errors in this procedure. One standard deviation has conservatively been estimated to be ±0.4 kJ/mol by taking plausible uncertainties of the many parameters of eqn (2) into account.

The fact that *sp* is 4.5(4) kJ/mol more stable than the *ac* form should be compared to the theoretical results. The MP2 prediction of this energy difference (Table 2) is best (4.0 kJ/mol), whereas B3LYP yielded 1.2 kJ/mol.

Discussion

The reason why the *sp* conformer is preferred over the *ac* form by as much as 4.5(4) kJ/mol is not obvious. Several forces seem to influence the conformational properties of ESE. It is possible that an interaction between the H4 atom and the π electron cloud of the triple bond of the nitrile group stabilizes *sp*, because the nonbonded distance between the H4 atom and the C7 atom is calculated from the MP2 structure of Table 1 to be 252 pm (MP2). The MP2 nonbonded distance between H4 and N8 is also as short as 276 pm. These values should be compared to the sum (290 pm) of Pauling's van der Waals radii[26] of hydrogen (120 pm) and the half thickness of an aromatic molecule (170 pm). A similar interaction is of course not possible in the *ac* form. Electron conjugation along the chain of the heavy atoms may also be favored in the *sp* rotamer as compared to the nonplanar *ac* rotamer, whereas the large C2−Se6−C7 angle (Table 1) in *sp* may indicate that repulsion between the vinyl and selenocyanate destabilizes this form.

It is interesting to compare the conformational properties of this selenocyanate ($H_2C{=}CHSeCN$) with similar thiocyanates such as $H_2C{=}CHSCN$ and $H_2C{=}C{=}CHSCN$. The conformational properties of $H_2C{=}CHSCN$[19,20] are very similar to those of $H_2C{=}CHSeCN$. The *sp* conformer of $H_2C{=}CHSCN$ is 3−6 kJ/mol more stable than the *ac*, and this conformer has a complicated fine structure of vibrational states associated with the torsion about the C−S bond, just as in the present case of ESE. The substitution of the sulfur atom with a selenium atom therefore seems to have little influence on the conformational and vibrational properties.

The conformational behavior of $H_2C{=}C{=}CHSCN$[27] is strikingly different from that of $H_2C{=}CHSCN$. Only one rotamer, the *ac*, characterized by a C−C−S−C dihedral angle of 134° was assigned for the former compound, and there is no evidence for an extremely low potential hump at the *ap* conformation (C−C−S−C dihedral angle equal to 180°). It remains to be seen whether the selenium analogue, $H_2C{=}C{=}CHSeCN$, behaves in a similar manner.

The predictions made by the B3LYP and MP2 calculations with the large aug-cc-pVTZ basis set are of mixed quality. The structure of the *sp* conformer seems to be relatively accurate, whereas the prediction of the structure of the *ac* form underestimates the C1−C2−Se6−C7 dihedral angle by 15−25°. Poor values are predicted for the quartic centrifugal distortion constants of *sp*, while a much better agreement is found for *ac*. The energy difference is well predicted by the MP2 procedure, whereas B3LYP performs more poorly.

Acknowledgment. We thank Anne Horn for her skillful assistance. The Research Council of Norway (program for supercomputing) is thanked for a grant of computer time. J.-C.G. thanks the CNES for financial support.

Supporting Information Available: Synthesis of etheneselenocyanate, MW spectra of the *ac* and *sp* conformers, and MP2 vibrational frequencies. This material is available free of charge via the Internet at http://pubs.acs.org.

References and Notes

(1) Sakaizumi, T.; Kohri, Y.; Ohashi, O.; Yamaguchi, I. *Bull. Chem. Soc. Jpn.* **1978**, *51*, 3411.
(2) Sakaizumi, T.; Obata, M.; Takahashi, K.; Sakaki, E.; Takeuchi, Y.; Ohashi, O.; Yamaguchi, I. *Bull. Chem. Soc. Jpn.* **1986**, *59*, 3791.
(3) Sakaizumi, T.; Itakura, T. *J. Mol. Spectrosc.* **1994**, *163*, 1.
(4) Bajor, G.; Veszpremi, T.; Riague, E. H.; Guillemin, J.-C. *Chem.-Eur. J.* **2004**, *10*, 3649.
(5) Møllendal, H.; Leonov, A.; de Meijere, A. *J. Phys. Chem. A* **2005**, *109*, 6344.
(6) Møllendal, H.; Cole, G. C.; Guillemin, J.-C. *J. Phys. Chem. A* **2006**, *110*, 921.
(7) Wodarczyk, F. J.; Wilson, E. B., Jr. *J. Mol. Spectrosc.* **1971**, *37*, 445.
(8) Frisch, M. J.; Trucks, G. W.; Schlegel, H. B.; Scuseria, G. E.; Robb, M. A.; Cheeseman, J. R.; Montgomery, J. A., Jr.; Vreven, T.; Kudin, K. N.; Burant, J. C.; Millam, J. M.; Iyengar, S. S.; Tomasi, J.; Barone, V.; Mennucci, B.; Cossi, M.; Scalmani, G.; Rega, N.; Petersson, G. A.; Nakatsuji, H.; Hada, M.; Ehara, M.; Toyota, K.; Fukuda, R.; Hasegawa, J.; Ishida, M.; Nakajima, T.; Honda, Y.; Kitao, O.; Nakai, H.; Klene, M.; Li, X.; Knox, J. E.; Hratchian, H. P.; Cross, J. B.; Adamo, C.; Jaramillo, J.; Gomperts, R.; Stratmann, R. E.; Yazyev, O.; Austin, A. J.; Cammi, R.; Pomelli, C.; Ochterski, J. W.; Ayala, P. Y.; Morokuma, K.; Voth, G. A.; Salvador, P.; Dannenberg, J. J.; Zakrzewski, V. G.; Dapprich, S.; Daniels, A. D.; Strain, M. C.; Farkas, O.; Malick, D. K.; Rabuck, A. D.; Raghavachari, K.; Foresman, J. B.; Ortiz, J. V.; Cui, Q.; Baboul, A. G.; Clifford, S.; Cioslowski, J.; Stefanov, B. B.; Liu, G.; Liashenko, A.; Piskorz, P.; Komaromi, I.; Martin, R. L.; Fox, D. J.; Keith, T.; Al-Laham, M. A.; Peng, C. Y.; Nanayakkara, A.; Challacombe, M.; Gill, P. M. W.; Johnson, B.; Chen, W.; Wong, M. W.; Gonzalez, C.; Pople, J. A. *Gaussian 03*, revision B.03; Gaussian, Inc.: Pittsburgh, PA, 2003.
(9) Møller, C.; Plesset, M. S. *Phys. Rev.* **1934**, *46*, 618.
(10) Becke, A. D. *Phys. Rev. A* **1988**, *38*, 3098.
(11) Lee, C.; Yang, W.; Parr, R. G. *Phys. Rev. B* **1988**, *37*, 785.
(12) Dunning, T. H., Jr. *J. Chem. Phys.* **1989**, *90*, 1007.
(13) Costain, C. C. *J. Chem. Phys.* **1958**, *29*, 864.
(14) Ray, B. S. *Z. Phys.* **1932**, *78*, 74.
(15) Watson, J. K. G. *Vibrational Spectra and Structure*; Elsevier: Amsterdam, 1977; Vol. 6.
(16) Oka, T.; Morino, Y. *J. Mol. Spectrosc.* **1961**, *6*, 472.
(17) Herschbach, D. R.; Laurie, V. W. *J. Chem. Phys.* **1964**, *40*, 3142.
(18) Oka, T. *J. Mol. Struct.* **1995**, *352/353*, 225.
(19) Beukes, J. A.; Klaeboe, P.; Møllendal, H.; Nielsen, C. J. *J. Mol. Struct.* **1995**, *349*, 37.
(20) Beukes, J. A.; Klaeboe, P.; Møllendal, H.; Nielsen, C. J. *J. Raman Spectrosc.* **1995**, *26*, 799.
(21) Esbitt, A. S.; Wilson, E. B. *Rev. Sci. Instrum.* **1963**, *34*, 901.
(22) Gwinn, W. D.; Gaylord, A. S. *Int. Rev. Sci.: Phys. Chem., Ser. 2* **1976**, *3*, 205.
(23) Marstokk, K.-M.; Møllendal, H.; Samdal, S.; Uggerud, E. *Acta Chem. Scand.* **1989**, *43*, 351.
(24) Wilson, E. B. Personal communication.
(25) Townes, C. H.; Schawlow, A. L. *Microwave Spectroscopy*; McGraw-Hill: New York, 1955.
(26) Pauling, L. *The Nature of the Chemical Bond*; Cornell University Press: New York, 1960.
(27) Møllendal, H.; Guillemin, J.-C. *J. Phys. Chem. A*, **2007**, *111*, 2542.